Surface Science 719 (2022) 122043

Contents lists available at ScienceDirect

Surface Science

journal homepage: www.elsevier.com/locate/susc

Spin coupling in Ag film growth on Sn/Ge(111)-$\sqrt{3} \times \sqrt{3}$

S. Starfelt, L.S.O. Johansson, H.M. Zhang *

Department of Engineering and Physics, Karlstad University, Karlstad SE-651 88, Sweden

ARTICLE INFO

Keywords:
Spin effects
Topological coupling: Thin films
Semiconductor: Interface structures
STM

ABSTRACT

Silver has been deposited on the Sn/Ge(111)-($\sqrt{3} \times \sqrt{3}$)-R30° surface at room temperature. The Ag growth and resulting surface morphology have been investigated using scanning tunneling microscopy. The first layer of silver forms an interface with domains of two different phases. One structure consists of short atomic rows with three-fold symmetry, oriented in the directions of the $\sqrt{3} \times \sqrt{3}$ surface. These rows are separated by a distance equal to $\sqrt{3}$ and are found to fit a $2\sqrt{3} \times \sqrt{3}$ unit cell. The other phase is a 3×3 honeycomb structure, oriented in the Ge(111) 1×1 directions. Atomic structural models for the two interface phases are proposed, based on two different spin arrangements of the Sn/Ge(111)-$\sqrt{3} \times \sqrt{3}$ surface. The results highlight the topological coupling of the two interface faces. Both interface structures are preserved with additional silver deposition. The second layer of Ag grows with a bulk-like lattice thickness on top of both interfaces. Low-energy electron diffraction on a mostly two layer Ag film reveals that it consists of domains where Ag grows in different orientations. These domains are rotated 30° with respect to each other, and thus mirror the symmetry directions of the two interfacial phases.

1. Introduction

Two-dimensional (2D) systems have historically received significant attention due to the interesting physical phenomena that arise in such systems. Examples of such phenomena are charge density waves and 2D superconductivity [2,1,3,4]. One type of such system is the adatom-induced $\sqrt{3} \times \sqrt{3}$ surface reconstructions on Si(111) and Ge (111), formed by deposition of 1/3 monolayer (ML) of Sn or Pb [5–7]. These surfaces are described with the T_4 adatom model, where the adatoms saturate the dangling bonds of the semiconductor surface, with only one dangling bond remaining on each adatom [8].

In particular, the Sn/Ge(111)-$\sqrt{3} \times \sqrt{3}$ surface has been the focus of a number of studies, as it has been shown to exhibit reversible $\sqrt{3} \times \sqrt{3} - 3 \times 3 - \sqrt{3} \times \sqrt{3}$ phase transitions when going from room temperature (RT) to temperatures below 30 K [9,10]. Additionally, the surface shows a 3×3 periodicity in the electronic structure at RT [8,11,12]. The origin of these phase transitions have been the source of some debate, with explanations including charge density wave formation and vertical shifts of the atomic positions in the lattice [9,13,14]. The ground state has been suggested as being driven by electronic correlations and magnetic effects, with proposals of both a Mott and a Slater insulator [10,15,16]. Similar to the Sn/Ge(111) case, the Sn/Si(111)-$\sqrt{3} \times \sqrt{3}$ surface has also been shown to have a low temperature phase transition, a $2\sqrt{3} \times \sqrt{3}$ ground state which involves a collinear antiferromagnetic spin ordering of the Sn atoms [17].

Another type of 2D system is Ag thin films on semiconductor surfaces, where the quantum size effects give rise to thickness modulation and oscillatory behavior of properties such as work function, adhesion and superconducting transition temperature [18–20]. Many of these effects are due to quantum well states (QWSs), discrete electronic energy states that have received significant attention in the past [21]. Quantum well states, along with electronic coupling effects, have also been shown to play a role for the film growth mode [22,23]. Recent studies have demonstrated the benefit of using the group III or group IV T_4 adatom $\sqrt{3} \times \sqrt{3}$ surfaces on Si(111) as a buffer layer for the growth of uniform Ag thin films on Si substrates [24–26]. This has allowed for the characteristics of QWSs to be explored for even thinner films than previously possible on Si substrates [27–29]. The Sn/Si(111) surface has shown to be particularly interesting, as it allows for layer-by-layer control of the film growth from the first layer of Ag. A natural extension of these studies is to move from Ag films on Sn/Si(111)-$\sqrt{3} \times \sqrt{3}$ to Ag films on Sn/Ge(111)-$\sqrt{3} \times \sqrt{3}$, which thus involves the combination of two 2D systems. As mentioned above, this combination presents an opportunity to study electronic coupling effects, and has the possibility of answering

* Corresponding author.
E-mail address: hanmin.zhang@kau.se (H.M. Zhang).

https://doi.org/10.1016/j.susc.2022.122043
Received 21 November 2021; Received in revised form 21 January 2022; Accepted 26 January 2022
Available online 31 January 2022

questions both about the Ag film growth and the ground state electronic structure of the Sn/Ge(111)-$\sqrt{3} \times \sqrt{3}$ surface itself.

This article presents a scanning tunnelling microscopy (STM) study of a novel system, Ag films grown on the Sn/Ge(111)-$\sqrt{3} \times \sqrt{3}$ surface at RT. The STM images show that the first layer of Ag forms an interface with two distinct phases, present in roughly equal amounts. One of these phases consists of short atomic-sized rows, which follow the direction of the Sn/Ge(111)-$\sqrt{3} \times \sqrt{3}$ surface. The other phase is a honeycomb structure, oriented in the Ge(111) 1×1 direction. Atomic models for the two interface phases are proposed, base on two different spin configurations of the Sn/Ge(111)-$\sqrt{3} \times \sqrt{3}$ surface. The first layer of Ag is thus shown to exhibit a topological behavior by locking the Sn/Ge(111) surface in a particular spin configuration. On top of both these interfaces, Ag grows as a fractured thin film. Small height corrugations on top of the Ag film, along with bordering unbroken interface, reveal that the interfacial structures are preserved beneath the film. Low-energy electron diffraction (LEED) confirms that the second layer of Ag grows with lattice parameters matching that of bulk Ag(111). The LEED images reveal two domains of the Ag film, rotated 30° with respect to each other, thus indicating that the two different interfacial phases produce Ag films in different directions. The results presented in this article clearly demonstrates how spin coupling can affect the film growth mode.

2. Experimental details

The experiments were performed in a two-chamber ultra-high vacuum (UHV) system from Omicron Nanotechnology GmbH. The analysis chamber was equipped with an Omicron variable temperature STM using a W/Ir tip, and a LEED. Base pressures in both chambers were $\sim 5 \times 10^{-11}$ mbar. Pressure during metal evaporations was below 3×10^{-10} mBar. The Ge(111) sample was n-type (Sb doped) with a resistivity of 0.2 Ωcm. The Ge(111)-c(2×8) surface was prepared in situ by a combination of cold and warm (Ar^+) sputtering, followed by annealing at 600 °C. The resulting surface was clean and well-ordered c (2×8), as confirmed by both LEED and STM. Approximately 0.4 ML of Sn was deposited onto the Ge(111)-c(2×8) surface followed by annealing at 300 °C for 2 min, in order to create a Sn/Ge(111)-$\sqrt{3} \times \sqrt{3}$ surface. Ag was evaporated from a Knudsen cell and deposited onto the Sn/Ge(111)-$\sqrt{3} \times \sqrt{3}$ surface while the sample was held at RT. Sn coverages are referenced with respect to the atomic density of Ge(111), whereas Ag coverages are referenced to that of Ag(111). The Ag desposition rate was calibrated using a quartz crystal thickness monitor along with previous film studies [26,29]. All measurements were performed at RT, and all STM biases are referenced with respect to the sample.

3. Results and discussion

3.1. LEED

The surface structure and quality were investigated using LEED. A well-defined $\sqrt{3} \times \sqrt{3}$ pattern can be seen in the LEED image shown in Fig. 1a, which was taken from the Sn/Ge(111)-$\sqrt{3} \times \sqrt{3}$ surface. Fig. 1b shows a LEED pattern taken from a surface consisting of mainly two layers of Ag film on Sn/Ge(111)-$\sqrt{3} \times \sqrt{3}$. This pattern introduces a number of new spots, while the $\sqrt{3} \times \sqrt{3}$ spots are no longer visible. The outer ones belong to a lattice constant of Ag(111) [30] (less than 2% error). These spots show two domains of Ag, rotated 30° from each other, one in the direction of the Ge(111) 1×1 and the other in the $\sqrt{3} \times \sqrt{3}$ direction. The spots has roughly the same intensity in both directions. The results thus indicate that the Ag film grows in domains with two different lattice orientations, in roughly equal proportions. This is contrary to most studies on Ag films on both Si and Ge, which typically has the Ag film oriented in the same direction as the underlying substrate (Si or Ge) [28,31]. The LEED image also shows a few spots inside of the Ge(111) 1×1 spots. These appear at positions expected from a $(2\sqrt{3} \times 2\sqrt{3})$-R30° pattern, even though many of the spots from such a pattern are missing. The origin of both the two domains of Ag and the inner spots will be explored further in the STM part of the paper.

3.2. STM

The surface structures and morphologies were investigated by STM. Fig. 2 shows the Sn/Ge(111)-$\sqrt{3} \times \sqrt{3}$ surface, where most of the surface constitutes of Sn atoms, along with a few defects in the form of darker appearing atoms. These correspond to Ge substitutional atoms. Both Sn and Ge belong to the same chemical group, but as the bonding length is shorter for Ge-Ge than Sn-Ge, the Ge substitutional atoms are expected to appear darker in STM images. The amount of substitutional atoms is less than 3%. The surface also has a few vacancies, which can be seen in the bottom right corner of Fig. 2a.

Fig. 3 shows STM images of the surface after deposition of 0.5 ML of Ag on the Sn/Ge(111)-$\sqrt{3} \times \sqrt{3}$ surface. Silver first grows as 1 ML islands, forming an interface, with little trace of 2 ML (as evident by Fig. 3c-3 d). The STM images show that the interface has two distinctly different structures (A and B), forming domains of roughly similar sizes.

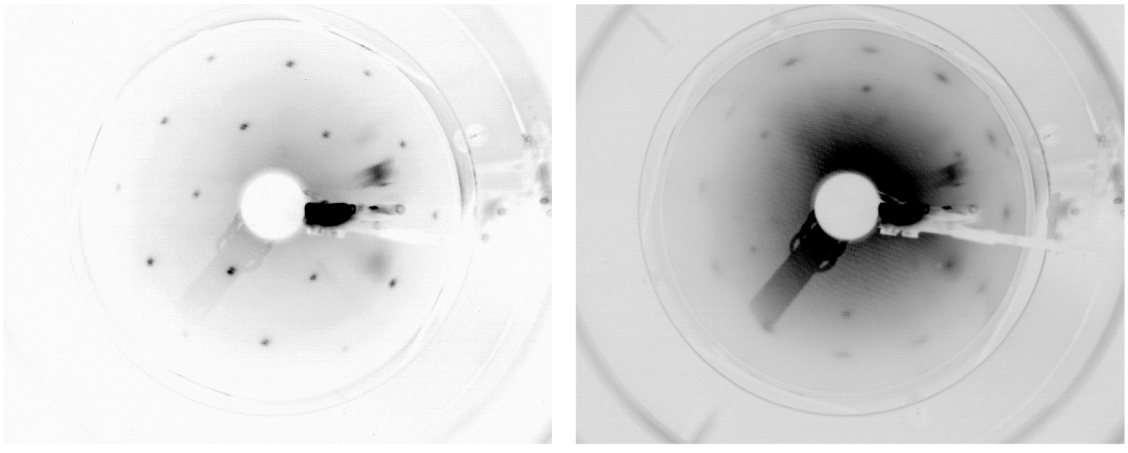

(a) (b)

Fig. 1. (a) LEED pattern of the prepared Sn/Ge(111)-$\sqrt{3} \times \sqrt{3}$ surface taken with 40 eV electron energy. (b) LEED pattern of a mostly two-layer Ag film (1.67 ML absolute coverage) taken with 63.1 eV electron energy.

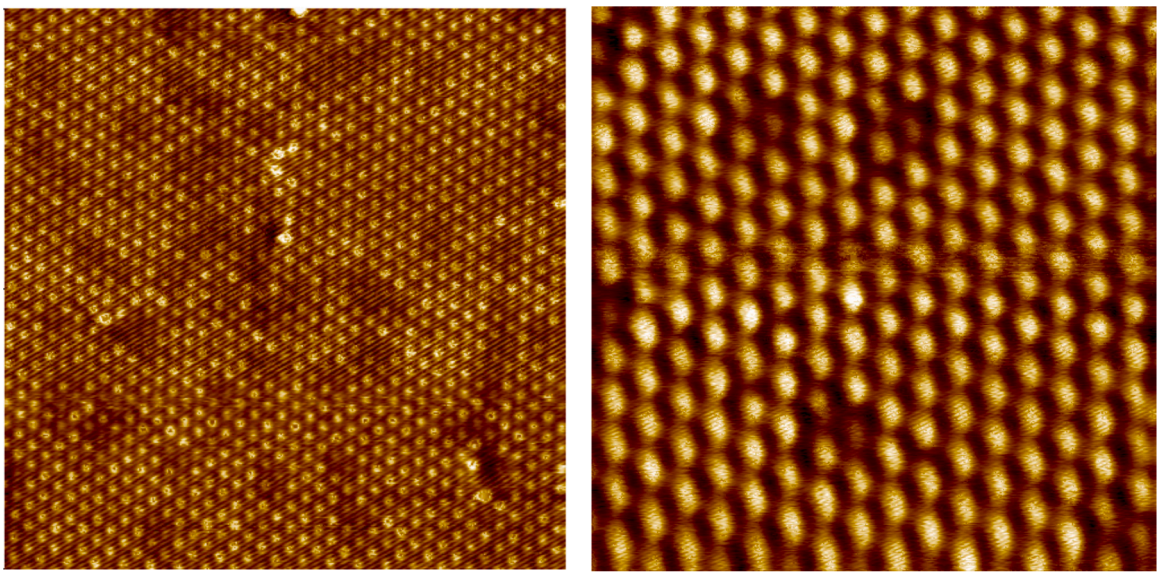

Fig. 2. STM images of the clean Sn/Ge(111)-$\sqrt{3} \times \sqrt{3}$ surface with bias, current and sizes values of (**a**) empty state, 2 V, 0.15 nA, 25 × 25 nm^2; (**b**) filled state 2 V, 0.05 nA, 10 × 10 nm^2.

This is in contrast to the Ag growth on Sn/Si(111)-$\sqrt{3} \times \sqrt{3}$, which has only a single phase [26]. One of the phases, which can be seen inside the circle marked with A in the empty-state image of Fig. 3a, consists of short atomic lines (or rows). Row structures are common for the Ag interfaces on metal-induced Si(111)-$\sqrt{3} \times \sqrt{3}$ surfaces [25,29]. The atomic row structures present for the Ag on Sn/Ge(111) differ from the Sn/Si(111) case in two important aspects. Firstly, the atomic rows on Sn/Ge(111) follow the $\sqrt{3} \times \sqrt{3}$ directions, which is evident when comparing against the uncovered Sn/Ge(111)-$\sqrt{3} \times \sqrt{3}$ surface area in Fig. 3. This is in contrast to Ag on Sn/Si(111), where the rows follow the underlying Si substrate 1 × 1 directions [26]. Secondly, the rows are separated by a distance equal to $\sqrt{3}$, which is shorter than the Ag on Sn/Si(111) case.

The other phase observed in the interface is a hexagonal honeycomb structure, seen inside the circle marked B in Fig. 3a. The honeycomb structure is also visible in the filled states image (Fig. 3b), but as an inverted image of the empty states (Fig. 3a). In the empty states, the border of the hexagon looks like a bright protrusion, whereas the middle of the hexagonal structure looks like a depression. The filled states however, show a large protrusion in the middle, surrounded by a thin depression which forms a hexagonal boundary. The honeycomb structure has a unit cell which is rotated 30° with respect to the $\sqrt{3} \times \sqrt{3}$ unit cell, meaning it follows the Ge(111) 1 × 1 directions. Fig. 3 shows that the size and shape of the honeycombs differs, with some appearing smaller and more deformed. Using the distance between the Sn atoms as reference, the most ordered (and most common) honeycomb unit cell fits a 3 × 3 periodicity.

The height of the line structure is roughly 2 Å above the $\sqrt{3} \times \sqrt{3}$ plane in both filled and empty states images. The honeycomb structure on the other hand, has a height of as low as 1.1 Å for some empty states biases, whereas the filled states show a height of 2 Å above the $\sqrt{3} \times \sqrt{3}$ plane. Electronic effects are thus more pronounced in the honeycomb structure than the line structure. The 2 Å filled-state heights indicate that both structures are mostly floating on top of the Sn $\sqrt{3} \times \sqrt{3}$ surface, which is especially evident for the line structure, where the Sn surface appears unbroken at the edges of the islands. The Ag interface does seem to alter the Sn/Ge(111)-$\sqrt{3} \times \sqrt{3}$ surface locally however, and these disturbances in turn causes large domains to form. This can be seen in, for example, the circle marked C in Fig. 3a. The Sn–Ag interaction of the two interfaces must therefore shift the positions of the Sn atoms slightly, which leads to the formation of domains that were not present before Ag deposition.

One question regarding the two phases is if one is a precursor to the other, formed by adding more Ag atoms on top of the other. To resolve this, more Ag were added to the sample. STM images of the surface with 1 ML coverage are shown in Fig. 4. The STM images show islands of 2 ML height on top of the 1 ML interface. These 2 ML islands form even as part of the surface still has patches of remaining Sn-$\sqrt{3} \times \sqrt{3}$ surface. This is in contrast to the Ag film growth on Sn/Si(111)-$\sqrt{3} \times \sqrt{3}$, where the second layer only started to grow after the whole surface was covered by the interface [26]. One explanation for this difference could be that the interface formation on Sn/Ge(111)-$\sqrt{3} \times \sqrt{3}$ shifts the positions of the Sn atoms and creates domain boundaries (see circle C in Fig. 3a), which prevents uniform film growth. The heights of the 2 ML islands vary with biases and measurement directions (depending on if referenced to the hexagonal or the line structure), but is approximately 2-2.5 Å, close to the distance between layers of bulk Ag(111) (2.36 Å)[30]. The height of the 2 ML Ag, along with the lattice constant calculated from LEED (Fig. 1b) indicates that starting from 2 ML, Ag grows as a bulk-like thin film. In Fig. 4, it is also evident that the 2 ML islands can grow on top of either interface phase. Fig. 4a shows a 2 ML island which is bordered by the honeycomb structure. In addition, traces of a hexagonal honeycomb structure can be faintly seen on top of the 2 ML surface. This is most likely small height corrugations caused by the interface beneath, another indication that the interface is preserved. Similar corrugations of the line structure can be seen on the 2 ML surface which is neighboring the atomic row interface phase (Fig. 4b). This also shows unbroken line structures bordering the 2 ML island. It therefore appears as if the 2 ML film can grow on top of either interface structure. This would explain the two domains of the Ag film observed in LEED (see Fig. 1b). As the two interface structures follow different directions, it is expected that the Ag films growing on top would do the same, i.e. form two domains rotated 30° with respect to each other.

Another interesting question is the atomic structures of the two interface phases. In the line structure, individual atoms are difficult to identify. However, as the distance between them is identical to that between Sn atoms in the $\sqrt{3} \times \sqrt{3}$ surface, the most likely scenario is

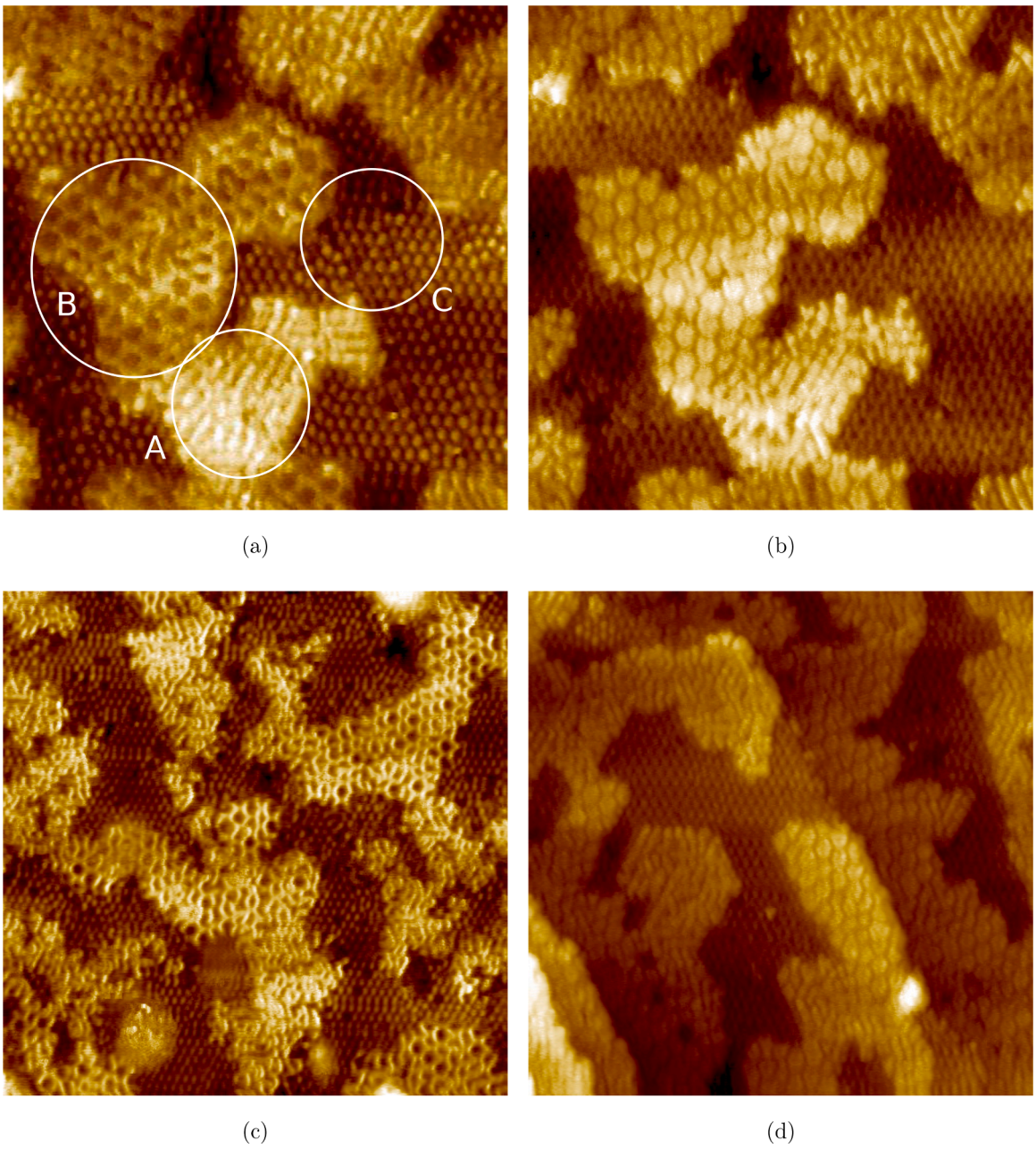

Fig. 3. STM images of 0.5 ML of Ag on Sn/Ge(111)-$\sqrt{3} \times \sqrt{3}$ with bias, current and sizes values of (**a**) empty state, 1.2 V, 0.3 nA, 30.1 × 30.1 nm^2; (**b**) filled states − 1 V, 0.3 nA, 30.1 × 30.1 nm^2; (**c**) empty state, 1.2 V, 0.15 nA, 50 × 50 nm^2; (**d**) filled state, − 1.5 V, 0.25 nA, 40 × 40 nm^2.

that the Ag atoms bond with the dangling bonds of the Sn atoms without breaking the Sn-Ge bonds and thus leave the Sn atomic placement in the surface mostly unaltered. Since the atomic rows are separated by a distance equal to $\sqrt{3}$, one would expect a $\sqrt{3} \times \sqrt{3}$ pattern still visible in the LEED image of the Ag film (Fig. 1b). However, the only additional pattern visible near the Ge(111) 1 × 1 spots belong to ($2\sqrt{3}$ × $2\sqrt{3}$)-R30°, with only a few of the spots visible. As the symmetry directions of ($2\sqrt{3} \times 2\sqrt{3}$)-R30° and ($\sqrt{3} \times \sqrt{3}$)-R30° are identical, the line structure should be the origin of the $2\sqrt{3} \times 2\sqrt{3}$ LEED pattern. The link between the LEED spots and the line structure will be explained further when discussing the atomic structure of the two interface phase.

The honeycomb structure appears a little more complicated. Fig. 5 shows STM images of the honeycomb structure with a smaller scan area than Fig. 3. It is clear that the largest unit cell is the most ordered, but that long-range ordering is somewhat disturbed for this interface phase. In Fig. 5a, the honeycomb structure is very clear, even though individual atoms are difficult to distinguish. Changing the bias slightly reveals more details of the atomic structure, as is evident in Fig. 5b. One particularly interesting feature is the protrusion in the middle of the honeycomb structure, which was not visible in Fig. 5a. While this protrusion is hardly visible in the empty states images, the filled states image (Fig. 5c) shows strong, spread out electron density in the middle of the hexagon. Furthermore, according to Fig. 5b, it appears as there is one protrusion at each corner of the hexagon, as well as another protrusion in between each corner.

As observed in the STM images, the largest and most symmetric hexagons are spaced apart by a 3 × 3 distance, which makes the electronic effects of the Sn/Ge(111)-$\sqrt{3} \times \sqrt{3}$ surface the most likely explanation for the honeycomb interface structure. There is overlap between a ($\sqrt{3} \times \sqrt{3}$)-R30° surface and a 3 × 3 honeycomb structure, achieved by placing the hexagon so that each corner is on top of a $\sqrt{3} \times$

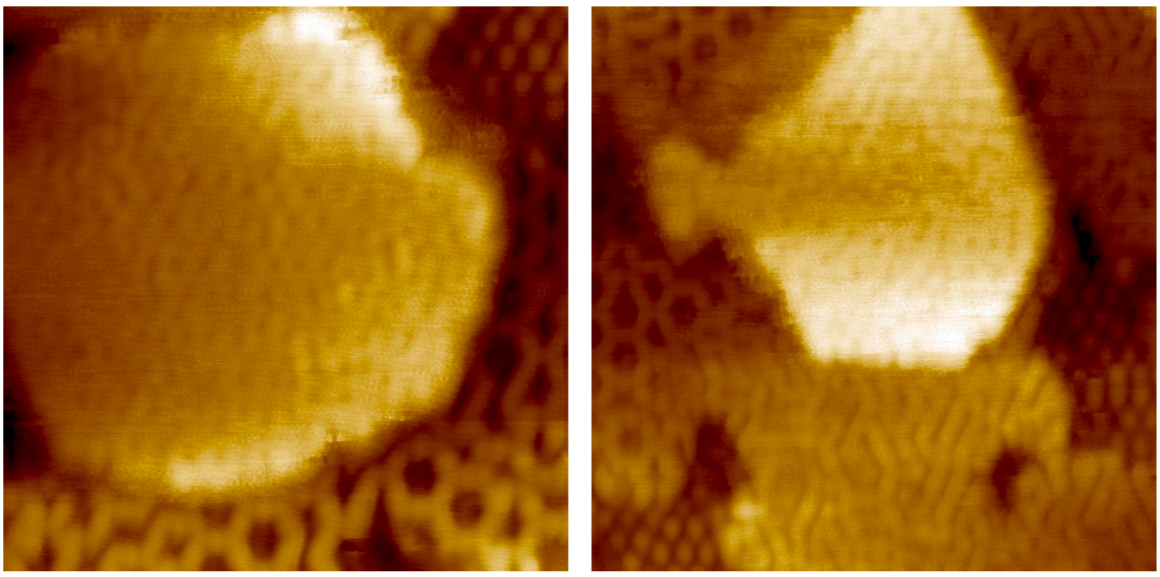

(a) (b)

Fig. 4. STM images of 1 ML of Ag on Sn/Ge(111)-$\sqrt{3} \times \sqrt{3}$ with bias, current and sizes values of (**a**) empty state 1.7 V, 0.2 nA, 15 × 15 nm^2; (**b**) empty state 1.7 V, 0.1 nA, 20.1 × 20.1 nm^2.

$\sqrt{3}$ atom. As the Sn/Ge(111)-$\sqrt{3} \times \sqrt{3}$ surface has a 3 ×3 electronic structure [8,11,12], which is also its LT phase, the interface structure could be explained by Ag bonding with each Sn atom and then adapting to the electronic landscape of the Sn/Ge(111)-$\sqrt{3} \times \sqrt{3}$ surface. The low temperature 3 × 3 phase of Sn/Ge(111) involves the Sn atoms being shifted slightly up or down and does indeed look like a honeycomb structure in STM, where the middle atom is brighter in the filled states and the surrounding hexagon brighter in the empty states [9]. This behavior matches very well with that of the interface in Fig. 5a and c. The lack of long-range ordering and broken unit cells observed in the STM images can be explained by surface defects such as Ge substitutional atoms. Any defect would locally break the 3 × 3 symmetry of the $\sqrt{3} \times \sqrt{3}$ surface, which in turn would affect the interface.

A more detailed picture of the suggested atomic structure can be seen in Fig. 6. It is important to note that this atomic structure lacks theoretical calculations, and that the atomic structures and number of atoms are crude estimates based on the experimental results. The honeycomb phase is based on a 3 × 3 surface. This is generated by starting from a Sn/Ge(111)-$\sqrt{3} \times \sqrt{3}$ surface and applying a 3 × 3 unit cell on top of it. According to a 3 × 3 model developed by Profeta and Tosatti [15], the 3 ×3 structure involves spin interactions, with a resulting ferrimagnetic surface. As the 3 × 3 unit cell contains 3 Sn atoms, two of these can be designated as spin up and one as spin down (see Fig. 6a). A model for the atomic structure of honeycomb phase can thus be created by placing Ag clusters (the triangles of three orange Ag atoms in Fig. 6a) on top of spin up and spin down Sn atoms, and Ag clusters (the pairs of green Ag atoms in Fig. 6a) between the spin-identical Sn atoms. This assignment of clusters fits well with the observed protrusions in Fig. 5b. The number of atoms in each cluster can be found by fitting to the estimated number of Ag atoms in a 3 × 3 unit cell. The experimentally obtained value for the complete interface layer was approximately 0.8 ML compared to bulk Ag (111). The ratio of atomic density for Ge(111)/Ag(111) is 0.52. Since a 3 × 3 unit cell of Ge(111) has 9 atoms, the number of Ag atoms should be $0.8/0.52 * 9$ which gives 13.77. A more theoretical approach would be to instead start from a 4 × 4 unit cell of Ag(111), which contains 16 atoms, but is 3.8% smaller than the 3 × 3 cell for Ge, which gives 16.6 atoms for the 3 × 3 unit cell. Removing the 3 Sn atoms that exist in the 3 ×3 cell, the theory thus gives a value of 13.6 Ag atoms per 3 × 3 unit cell. As the experimental and the theoretical values match, it is possible to conclude that the number of Ag atoms in the 3 × 3 unit cell should be around 14. In order to reach a spin-neutral unit cell, the Ag clusters on top of the Sn atoms has to contain an odd number of Ag atoms, whereas those in between the spin-up Sn atoms should have an even number of Ag atoms. For the honeycomb structure, a spin neutral surface with the right amount of atoms can be achieved by placing 3 atoms in the Ag cluster on top of the Sn atoms and 2 Ag atoms in the clusters between the spin-identical Sn atoms. This assignment will give 15 atoms for the 3 × 3 unit cell, which is close to the expected value from the calculations above.

Moving to the dynamic picture, the 3 × 3 electronic structure of Sn/Ge(111)-$\sqrt{3} \times \sqrt{3}$, while being the ground state, is only visible for low temperatures. At RT, the 3 × 3 phase of the surface is removed, as the thermal energy allows for the positions of the Sn atoms to fluctuate. However, the spins of the Sn atoms could still be linked with each other, so that incoming Ag atoms can interact with the entire spin network in order to remove the spin polarization of the surface. This is achieved by the cluster of Ag atoms taking the opposite spin of the Sn atoms, thereby creating a spin neutral surface. The Ag interface thus allows for the Sn atoms in the Sn/Ge(111)-$\sqrt{3} \times \sqrt{3}$ surface to be locked in their ground state even at RT.

The atomic structure of the interfacial line phase is a little harder to determine due to the difficulty of resolving individual protrusions along the rows. In the model proposed for the honeycomb phase, Ag clusters that lie between Sn atoms were limited to those locations where the neighboring Sn atoms have the same spin. Since the most common length of the atomic rows were close to an integer value of $2\sqrt{3}$, the line structure would consist of Ag clusters on top of 3 Sn atoms, with possibly extra Ag clusters between the Sn atoms with the same spins. Assuming the clusters are filled in a like manner as the honeycomb structure (3 atoms on top of Sn and 2 atoms between), the number of Ag atoms in a $2\sqrt{3} \times 2\sqrt{3}$ unit cell will be 20, which is identical atomic density to the honeycomb phase.

A question is why the line phase would form at all. In the proposed model for the honeycomb phase, Ag clusters that bind to locations between two Sn atoms only do so when the neighboring Sn has the same spin. However, using the same 3 × 3 spin cell for the line structure as the honeycomb phase, an atomic row which involves 3 Sn atoms would necessarily involve two different spins, thus making it hard for Ag

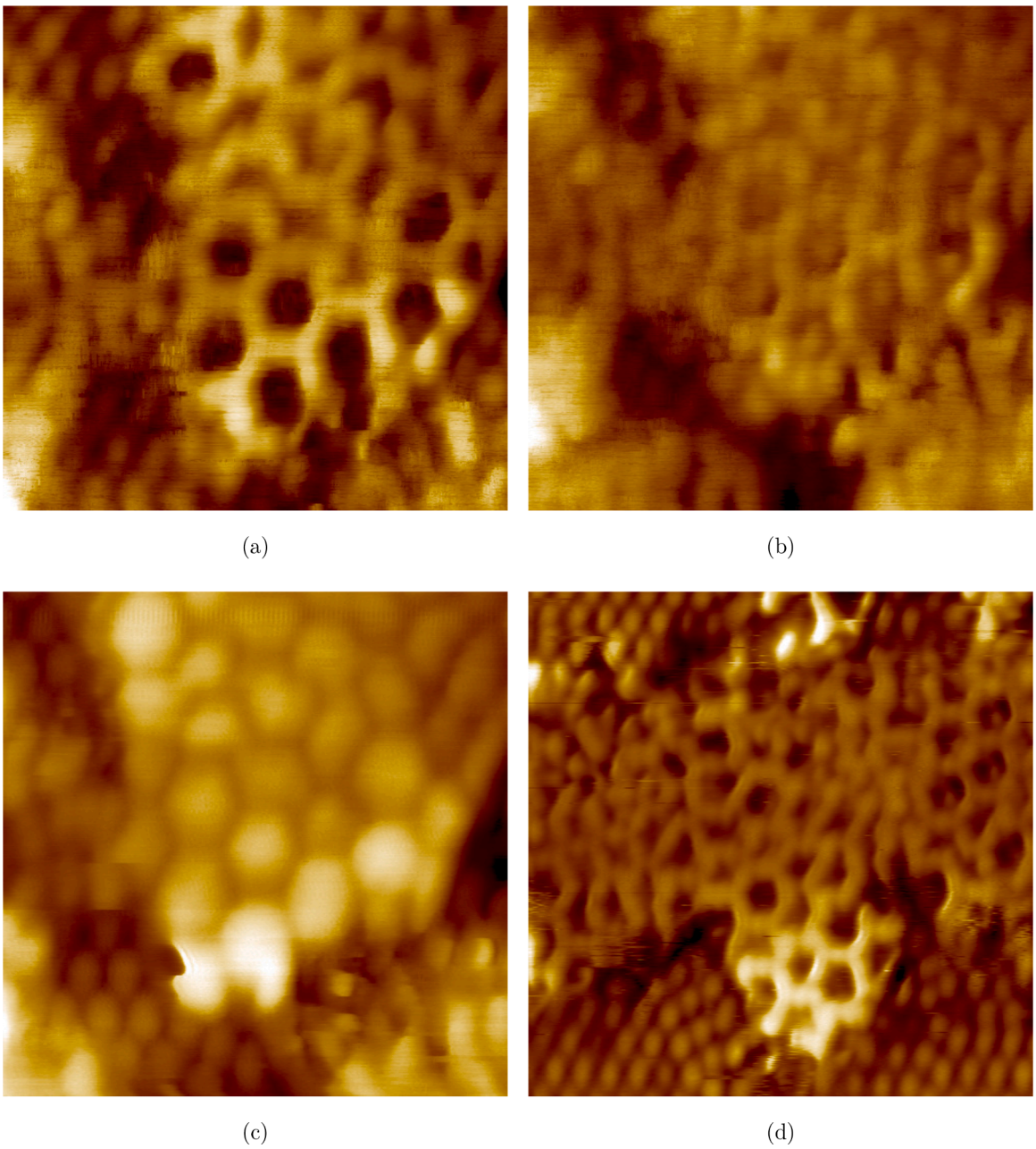

Fig. 5. STM images of 0.5 ML of Ag on Sn/Ge(111)-$\sqrt{3} \times \sqrt{3}$ with bias, current and sizes values of (**a**) empty state, 1.5 V, 0.15 nA, 9.97 $\times$ 9.97 nm^2; (**b**) empty state, 2 V, 0.15 nA, 9.97 $\times$ 9.97 nm^2; (**c**) filled state, $-$ 2 V, 0.15 nA, 9.97 $\times$ 9.97 nm^2; (**d**) empty state, 1.5 V, 0.15 nA, 15.3 $\times$ 15.3 nm^2.

clusters to fill up the spaces between the Sn atoms. Recent studies on the insulating ground state of the neighboring Sn/Si(111)-$\sqrt{3} \times \sqrt{3}$ system has proposed a collinear antiferromagnetic $2\sqrt{3} \times \sqrt{3}$ ordering of the spins, with 120° rotational symmetry leading to an effective $2\sqrt{3} \times 2\sqrt{3}$ surface Brillouin zone [17,32]. This arrangement of Sn atoms fits well with the line structure, which can be seen in Fig. 6b. As the Sn/Si(111) and Sn/Ge(111) systems are similar, it is possible that a similar arrangement could be favored even for the Sn/Ge(111)-$\sqrt{3} \times \sqrt{3}$ surface. This would make the line phase a $2\sqrt{3} \times \sqrt{3}$ structure, which is 120° rotationally symmetric. Including all three domains, a $2\sqrt{3} \times \sqrt{3}$ structure would give rise to an identical LEED pattern as a $2\sqrt{3} \times 2\sqrt{3}$ structure, thus explaining the faint $(2\sqrt{3} \times 2\sqrt{3})$-R30° pattern that was visible in LEED (Fig. 1b). Another mechanism behind the formation of the line structure would be to start from the dynamic picture of the 3×3 spin order used for the honeycomb phase. At RT, the spin of the Sn atoms is not fixed in the ground state and as such there may be times when short lines are formed where the Sn atoms have the same spin. Once incoming Ag atoms bind to the Sn atoms and form a cluster, the spins of the Sn atoms become locked in place. In this case, Ge substitutional atoms might make it easier for the line structure to form, as their spin coupling with the surrounding Sn atoms would be less strong and thus make it easier for the Ge atoms to fit into any row. Due to the three-fold symmetry of the unit cell, it is expected that there would be intersections between two or more atomic rows with the same spin configuration that are oriented in different directions. Consistently with the proposed model, Ag clusters of two atoms should be able to bond between the lines at these locations, thus creating a zig-zag pattern. Such a zig-zag pattern can indeed be seen in some locations in the STM images of the interface (Figs. 3 and 4).

The orientation of Ag atoms in the clusters is very difficult to determine directly from the STM images. A likely scenario is that the Ag

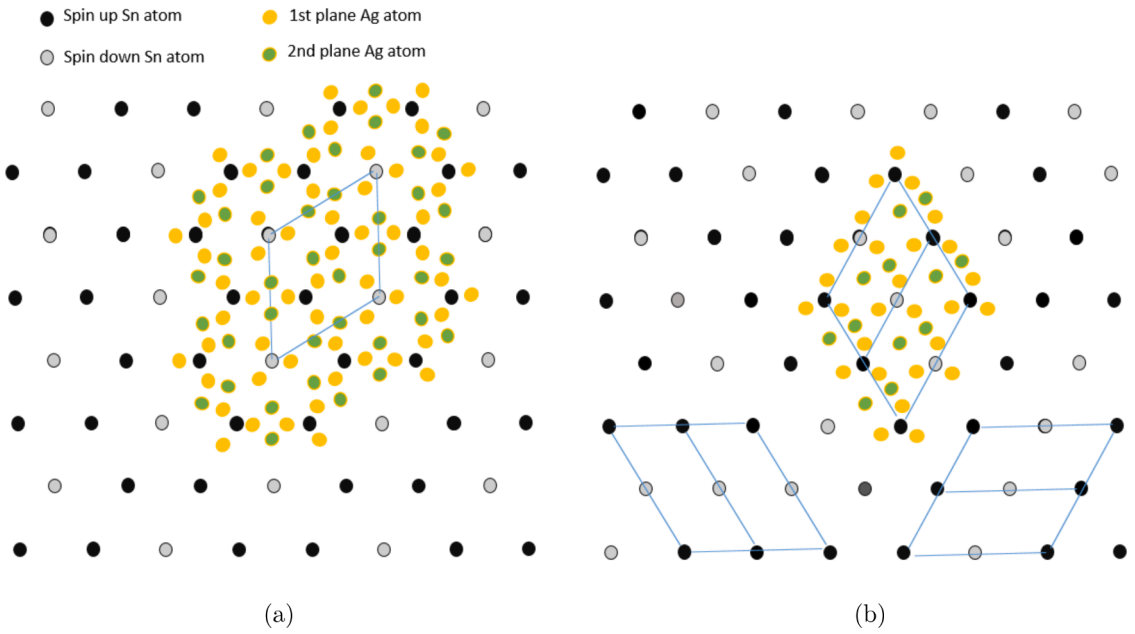

Fig. 6. Schematic overview of the atomic structure of the two interface phases, (**a**) the honeycomb structure and (**b**) the line structure. The blue lines mark the unit cells, which in (a) is 3×3 and in (b) $2\sqrt{3} \times \sqrt{3}$. In (b), rotationally symmetric unit cells without Ag atoms are also marked. (For interpretation of the references to color in this figure legend, the reader is referred to the web version of this article.)

clusters consisting of 3 atoms would have a triangular arrangement of the atoms, centered on the Sn atoms in the $\sqrt{3} \times \sqrt{3}$ surface. Using the distance between Ag atoms in the (111) plane as the minimum distance allowed between two Ag atoms, it is thus impossible to add the Ag clusters consisting of 2 atoms in the same plane as the clusters of 3 atoms, if they are all to fit in between the Sn atoms. The model proposed here thus places the clusters of 2 Ag atoms at a different horizontal plane than the 3 atom clusters.

The atomic models of the two interface phases are based on spin coupling, as it has previously been used to explain the low temperature phase transitions of the Sn/Ge(111)-$\sqrt{3} \times \sqrt{3}$ surface. While other explanations for the two interface phases may be possible, they have to take into account the fact that Ag clusters bind to sites in-between some Sn atoms, but not others. This is not possible unless there is something that differentiates the Sn atoms in the $\sqrt{3} \times \sqrt{3}$ surface. Using spin as the differentiating factor, along with the two different spin configurations, naturally produces the two interface structures. This strengthens the conclusion that spin effects of the Sn/Ge(111)-$\sqrt{3} \times \sqrt{3}$ surface is the best explanation for the origin of the two interface phases. Furthermore, these results highlight the topological coupling of the first layer Ag interface.

Fig, 7 shows STM images of the surface after deposition of a total of 1.67 ML of Ag. This number was chosen in an attempt to reach a two layer thick film, as previous studies on Ag films on $\sqrt{3} \times \sqrt{3}$ Si(111)

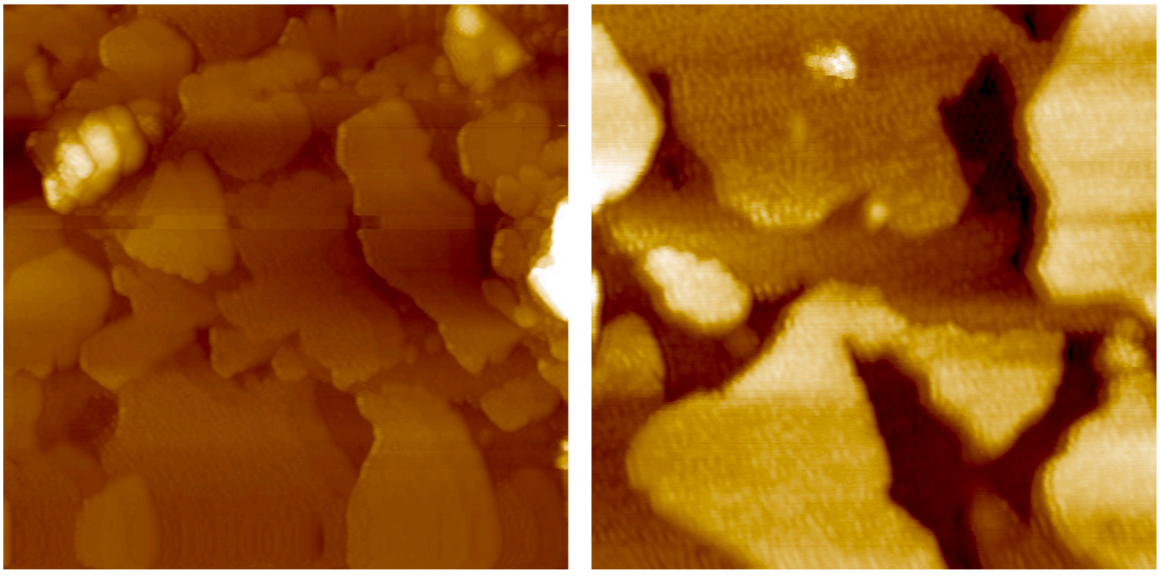

Fig. 7. STM images of 1.67 ML of Ag on Sn/Ge(111)-$\sqrt{3} \times \sqrt{3}$ with bias, current and sizes values of (**a**) filled state, -2 V, 0.1 nA, 100×100 nm^2; (**b**) filled state, -1.7 V, 0.05 nA, 50×50 nm^2.

surfaces has shown that the first layer of Ag requires less silver than the subsequent ones [25,26,29], and this was assumed to be the case also for Ag on Sn/Ge(111). The STM images show patches where the third layer starts to grow before the second layer fully covers the surface. The images also show places where the 2 ML islands have boundaries with each other without growing together into a smooth film. This is expected from a surface where the film grows in domains with 30° rotations, as was shown by LEED (Fig. 1). The two interface structures thus serves to create domains which are preserved on further Ag deposition, which decouples parts of the surface from each other, so that only local layer-by-layer growth can be expected. The distance between the second and third layer is roughly 2.4 Å, almost identical to the bulk value (2.36 Å) [30]. The fact that Ag deposition on the Sn/Ge(111)-$\sqrt{3} \times \sqrt{3}$ surface generates two types of interface structures where both allow for Ag film growth, provides a novel system for studying quantum size effects and thin film growth. Additionally, the two interfacial phases can provide further insight into the electronic structure of the Sn/Ge(111)-$\sqrt{3} \times \sqrt{3}$ surface.

This study leaves several open questions, which require further studies to answer. Deposition of Ag at different sample temperatures would give insight into temperature variation in the ratio of the two interface phases and could thus point to one or the other being the ground state. Theoretical calculations or modeling of the atomic structure are needed in order to develop the atomic model. Furthermore, spin-resolved photoemission or spin-resolved STM would be highly useful in order to confirm the suggested spin structure of the system.

4. Conclusions

Silver thin film growth on Sn/Ge(111)-$\sqrt{3} \times \sqrt{3}$ have been investigated using LEED and STM, where Ag was deposited at room temperature. The first layer of Ag forms an interface consisting of domains with two different structures. These two phases are short atomic rows and a honeycomb structure, respectively. The atomic rows have a three-fold symmetry and are oriented in the direction of the Sn/Ge(111)-$\sqrt{3} \times \sqrt{3}$ surface. They are separated by a distance equal to the $\sqrt{3}$ length of the Ge(111) 1×1 surface unit vectors, and found to have a unit cell of $2\sqrt{3} \times \sqrt{3}$. The honeycomb phase has a 3×3 structure, oriented in the direction of the underlying Ge substrate. Atomic models of the two interfacial phases are proposed, based on two different spin configurations of the Sn/Ge(111)-$\sqrt{3} \times \sqrt{3}$ surface. The model places clusters of 3 Ag atoms on top of each Sn atom, as well as clusters of 2 Ag atoms in between spin-identical Sn atoms. The results show the topological coupling of the first Ag layer. Both interface phases are preserved below the second layer of Ag, which grows with bulk-like lattice parameters. The resulting Ag film has domains where the film is oriented either in the direction of Ge(111) 1×1 or along the $\sqrt{3} \times \sqrt{3}$ directions, most likely generated by the two interfaces. The presence of two interface structures makes this a novel system and opens up the possibility to further study Ag film growth and interface related effects, as well as the Sn/Ge(111)-$\sqrt{3} \times \sqrt{3}$ surface itself.

Author statement

The authors do not wish to provide a detailed author statement at this point.

Declaration of Competing Interest

Authors declare that they have no conflict of interest.

References

[1] J. Carpinelli, H. Weitering, E. Plummer, et al., Nature 381 (1996) 398.
[2] H.H. Weitering, J.M. Carpinelli, A.V. Melechko, J. Zhang, M. Bartkowiak, E. W. Plummer, Science 285 (5436) (1999) 2107–2110, https://doi.org/10.1126/science.285.5436.2107.
[3] T. Zhang, P. Cheng, W. Li, et al., Nat. Phys. 6 (2010) 104.
[4] C. Brun, T. Cren, V. Cherkez, Nat. Phys. 10 (2014) 444.
[5] J. Lobo, A. Tejeda, A. Mugarza, E.G. Michel, Phys. Rev. B 68 (2003) 235332, https://doi.org/10.1103/PhysRevB.68.235332.
[6] I. Brihuega, O. Custance, R. Pérez, J.M. Gómez-Rodríguez, Phys. Rev. Lett. 94 (2005) 046101, https://doi.org/10.1103/PhysRevLett.94.046101.
[7] M. Månsson, O. Tjernberg, M. Göthelid, M. Grishin, T. Claesson, U. Karlsson, Surf. Sci. 602 (5) (2008) L33–L37, https://doi.org/10.1016/j.susc.2008.01.015.http://www.sciencedirect.com/science/article/pii/S0039602808000393
[8] R.I.G. Uhrberg, H.M. Zhang, T. Balasubramanian, Phys. Rev. Lett. 85 (2000) 1036–1039, https://doi.org/10.1103/PhysRevLett.85.1036.
[9] J.M. Carpinelli, H.H. Weitering, M. Bartkowiak, R. Stumpf, E.W. Plummer, Phys. Rev. Lett. 79 (1997) 2859–2862, https://doi.org/10.1103/PhysRevLett.79.2859.
[10] R. Cortés, A. Tejeda, J. Lobo, C. Didiot, B. Kierren, D. Malterre, E.G. Michel, A. Mascaraque, Phys. Rev. Lett. 96 (2006) 126103, https://doi.org/10.1103/PhysRevLett.96.126103.
[11] R.I.G. Uhrberg, T. Balasubramanian, Phys. Rev. Lett. 81 (1998) 2108–2111, https://doi.org/10.1103/PhysRevLett.81.2108.
[12] J. Ortega, R. Pérez, F. Flores, J. Phys. 14 (24) (2002) 5979–6004, https://doi.org/10.1088/0953-8984/14/24/307.
[13] A. Goldoni, S. Modesti, Phys. Rev. Lett. 79 (1997) 3266–3269, https://doi.org/10.1103/PhysRevLett.79.3266.
[14] F. Ronci, S. Colonna, S.D. Thorpe, A. Cricenti, G. Le Lay, Phys. Rev. Lett. 95 (2005) 156101, https://doi.org/10.1103/PhysRevLett.95.156101.
[15] G. Profeta, E. Tosatti, Phys. Rev. Lett. 98 (2007) 086401, https://doi.org/10.1103/PhysRevLett.98.086401.
[16] J.-H. Lee, H.-J. Kim, J.-H. Cho, Phys. Rev. Lett. 111 (2013) 106403, https://doi.org/10.1103/PhysRevLett.111.106403.
[17] M. Jäger, C. Brand, A.P. Weber, M. Fanciulli, J.H. Dil, H. Pfnür, C. Tegenkamp, Phys. Rev. B 98 (2018) 165422, https://doi.org/10.1103/PhysRevB.98.165422.
[18] J. Paggel, C. Wei, M. Chou, D.-a. Luh, T. Miller, T.-C. Chiang, Phys. Rev. B 66 (23) (2002) 1–4, https://doi.org/10.1103/PhysRevB.66.233403.
[19] T.Z. Han, G.C. Dong, Q.T. Shen, Y.F. Zhang, J.F. Jia, Q.K. Xue, Appl. Phys. Lett. 89 (18) (2006).
[20] Y. Guo, Y.-F. Zhang, X.-Y. Bao, et al., Science 306 (5703) (2004) 1915–1917.
[21] T.C. Chiang, Surf. Sci. Rep. 39 (7) (2000) 181–235.
[22] Z. Zhang, Q. Niu, C.-K. Shih, Phys. Rev. Lett. 80 (1998) 5381.
[23] B. Wu, Z. Zhang, Phys. Rev. B 77 (2008) 035410.
[24] J.-H. He, L.-Q. Jiang, J.-L. Qiu, L. Chen, K.-H. Wu, Chin. Phys. Lett. 31 (12) (2014) 128102.
[25] S. Starfelt, L.S.O. Johansson, H.M. Zhang, Surf. Sci. 682 (2019) 25–32.
[26] S. Starfelt, R. Lavén, L.S.O. Johansson, H.M. Zhang, Surf. Sci. 701 (2020) 121697, https://doi.org/10.1016/j.susc.2020.121697.
[27] H.M. Zhang, L.J. Holleboom, L.S.O. Johansson, Phys. Rev. B 96 (2017) 041402.
[28] S. Starfelt, H.M. Zhang, L.S.O. Johansson, Phys. Rev. B 97 (2018) 195430.
[29] S. Starfelt, L.S.O. Johansson, H.M. Zhang, Surf. Sci. 692 (2020) 121531, https://doi.org/10.1016/j.susc.2019.121531.
[30] A. Arranz, J.F. Sanchez-Royo, J. Avila, V. Perez-Dieste, P. Dumas, M.C. Asensio, Phys. Rev. B 65 (19) (2002) 195410.0106104
[31] P. Moras, G. Bihlmayer, E. Vescovo, P.M. Sheverdyaeva, M. Papagno, L. Ferrari, C. Carbone, J. Phys. 29 (49) (2017) 495806.
[32] G. Li, P. Höpfner, J. Schäfer, et al., Nat. Commun. 4 (2013) 1620.